

Effect of TiO₂ nanotube length and lateral tubular spacing on photovoltaic properties of back illuminated dye sensitized solar cell

SHANTIKUMAR V NAIR*, A BALAKRISHNAN, K R V SUBRAMANIAN, A M ANU, A M ASHA and B DEEPIKA

Nano Solar Division, Amrita Centre for Nanosciences, Kochi 682 041, India

MS received 28 February 2011; revised 19 May 2011

Abstract. The main objective of this study is to show the effect of TiO₂ nanotube length, diameter and intertubular lateral spacings on the performance of back illuminated dye sensitized solar cells (DSSCs). The present study shows that processing short TiO₂ nanotubes with good lateral spacings could significantly improve the performance of back illuminated DSSCs. Vertically aligned, uniform sized diameter TiO₂ nanotube arrays of different tube lengths have been fabricated on Ti plates by a controlled anodization technique at different times of 24, 36, 48 and 72 h using ethylene glycol and ammonium fluoride as an electrolyte medium. Scanning electron microscopy (SEM) showed formation of nanotube arrays spread uniformly over a large area. X-ray diffraction (XRD) of TiO₂ nanotube layer revealed the presence of crystalline anatase phases. By employing the TiO₂ nanotube array anodized at 24 h showing a diameter ~80 nm and length ~1.5 μm as the photo-anode for back illuminated DSSCs, a full-sun conversion efficiency (η) of 3.5 % was achieved, the highest value reported for this length of nanotubes.

Keywords. TiO₂; back illumination; dye-sensitized solar cell; nanotubes.

1. Introduction

In dye sensitized solar cells (DSSC), photo-anodes based on TiO₂ nanotubes offer a tremendous opportunity to make use of the near-infrared region of the solar spectrum with improved electron transfer, primarily because of their aligned geometry and their consequent ability to serve as efficient current collectors and transporters (Paulose *et al* 2007; Liu *et al* 2008). There are a few reported methods for obtaining long TiO₂ nanotube arrays (lengths in the range 10–100 μm) on ITO/FTO (indium/fluorine doped tin oxide) glass substrate as photoanodes (Tang *et al* 2008; Varghese *et al* 2009). Studies have shown that TiO₂ thin films deposited on Ti substrates are appropriate for constructing back-illuminated DSSCs (Tao *et al* 2010). Also, depositing TiO₂ nanotubes on Ti substrates is an easily scaled-up approach and relevant to the low-cost fabrication of back-illuminated DSSCs. It has been reported that in back illuminated DSSCs (Park *et al* 2000; Paulose *et al* 2006), the charge collection and light-harvesting efficiencies are 20 and 25 % higher, respectively than corresponding nanoparticle based front illuminated DSSCs. Inspired by this, in the present study, vertically aligned and uniform sized TiO₂ nanotubes of different lengths have been fabricated directly onto a Ti plate under controlled anodization conditions. It was found that for an anodization time of 24 h, TiO₂ nanotubes of diameter ~80 nm and length ~1.5 μm was obtained which showed good inter-tubular lateral spacings. By employing these

nanotubes as photoanodes in a back illuminated DSSC model, an overall light to electricity conversion efficiency of 3.5% was achieved, which is the highest reported value for this tube length. Figure 1 compares the cell efficiency with other studies for back illuminated DSSCs as a function of TiO₂ tube length for a given diameter (D) (Park *et al* 2000; Jennings *et al* 2008; Roy *et al* 2010). We had also fabricated TiO₂ nanotubes of different lengths and employed them as photoanodes in back illuminated DSSCs. It was seen that forming long, dense TiO₂ tubular network can limit the

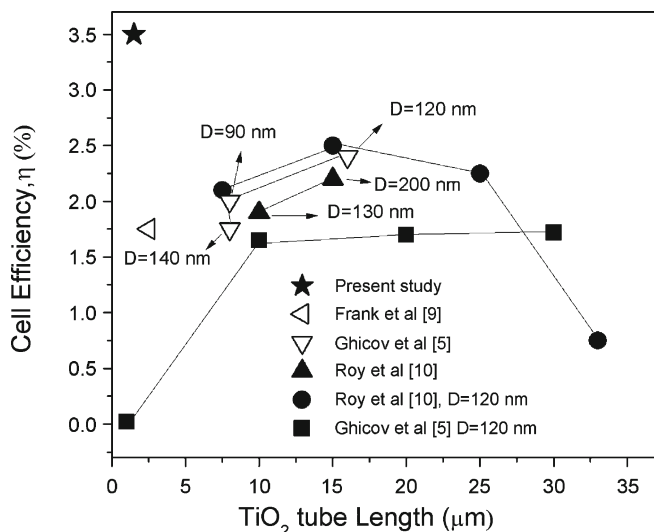


Figure 1. Comparison of our cell efficiency data with other studies (Park *et al* 2000; Jennings *et al* 2008; Roy *et al* 2010).

* Author for correspondence (shantinair@aims.amrita.edu)

chances of dye wetting to TiO₂, thereby reducing the overall cell efficiency. This study also brings out the importance of intertubular lateral spacings, which could also play a crucial role in determining the dye wetting with TiO₂ and improving the cell efficiency in DSSCs.

2. Experimental

All chemicals were of analytical grade reagent (Sigma Aldrich) and used without further purification. Commercially pure titanium plates (98%, grade 2, 14 × 14 × 1 mm) were used as anode. These Ti plates were polished with SiC 120–1200 grit abrasive paper and cleaned ultrasonically with acetone and dried at 40 °C in air. Electrolyte consisting of 7 vol. % of ethylene glycol and 3 vol. % of ammonium fluoride was used. Ti plate and platinum rod were taken as working and counter electrode, respectively. The anodization process was carried out under controlled conditions of 24, 36, 48 and 72 h at an applied voltage of 40 V. The anodized plates were annealed at 450 °C for 30 min. Morphological and phase analysis for the obtained nanotubes were done by using scanning electron microscopy (SEM, Model: JEOL JSM-6490 LA) and X-ray diffraction analysis (XRD, XPert PRO Analytical), respectively. Image J software was used to determine the length, diameter size distribution (DSD) and lateral space distribution (LSD) of these nanotubes. For each

anodization condition, three samples were prepared. Prior to the solar cell assembly, two sets of TiO₂ photo-anodes were prepared. One set was treated with TiCl₄ solution at 60 °C for 30 min and the other was left untreated. These photo-anodes were soaked in 0.3 mM of ruthenium (II) dye (N719, Solaronix) in acetonitrile and *t*-butanol (1:1) solution for 48 h and coupled with a platinized counter electrode. The two electrodes were clipped together and the internal space of the cell was filled with electrolyte. The electrolyte composed of 0.6M BMII (butyl-methyl-imidazolium iodide), 0.03M I₂, 0.1M guanidium thiocyanate and 0.5M tert-butyl pyridine in a solution mixture of 85 vol% acetonitrile and 15 vol% valeronitrile. The photocurrent–voltage (*I*–*V*) characteristics of the coupled solar cells were measured under one sun illumination of a solar simulator (Newport, Oriol Class-A). The illumination was done from the platinized counter electrode side (area exposed was 0.5 cm²). Photocurrent density (*J*_{sc}) and open-circuit voltage (*V*_{oc}) were measured using Keithley 2400 digital source meter under an applied external potential scan.

3. Results and discussion

Figure 2a shows highly oriented TiO₂ nanotube arrays formed on the Ti substrate. The average length of the nanotube was estimated as 1.5 ± 0.3 μm (figure 2b).

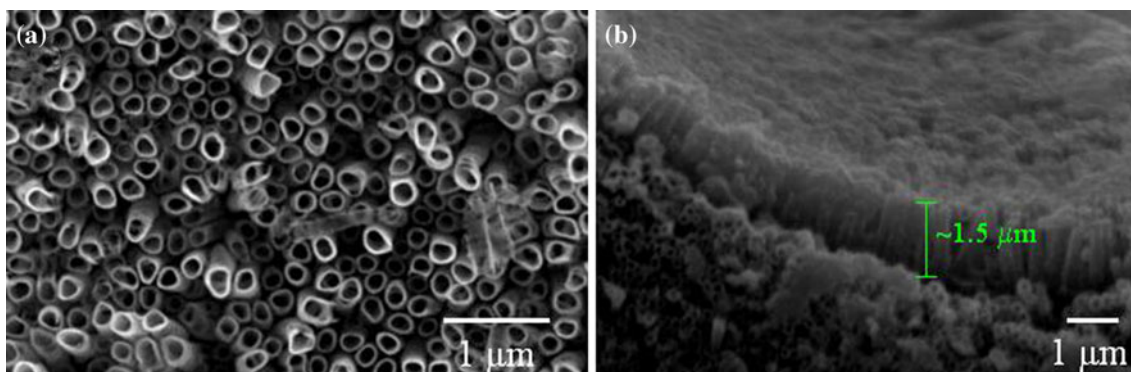


Figure 2. SEM image of TiO₂ nanotubes (a) top and (b) side view (cleaved plate).

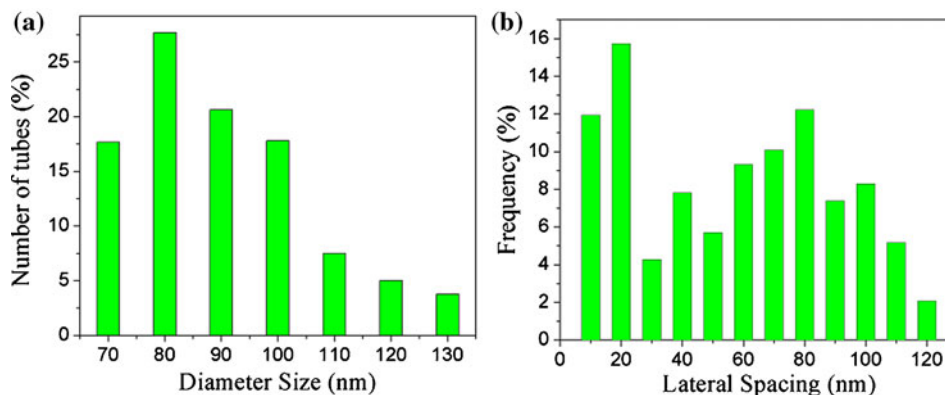
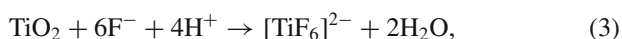
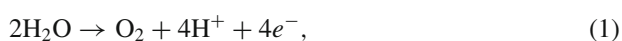


Figure 3. (a) DSD and (b) LSD profile of nanotubes.

Figure 3a shows DSD analysis of TiO₂ nanotubes exhibiting narrow skewed distribution in the range 70–130 nm, centred at ~80 nm. The analysis of lateral spacing distribution (LSD) (figure 3b) showed a multi-modal distribution ranging from 10–120 nm, indicating that there was good lateral spacing/opening between the nanotubes, which could enhance the dye–TiO₂ interaction. XRD patterns (figure 4) of the nanotube layer (post annealing) revealed presence of anatase phase. XRD patterns (figure 4) of the nanotube layer (post annealing) revealed presence of anatase phase, with no secondary crystalline phases. The formation of TiO₂ nanotubes in fluoride containing electrolytes has been discussed in detail in our earlier work (Anitha *et al* 2010). Briefly to state, the formation of TiO₂ nanotubes is attributed to three simultaneously occurring processes: field assisted oxidation of Ti metal to form TiO₂, field assisted dissolution of Ti metal to form TiO₂ and chemical dissolution of Ti and TiO₂ due to etching by fluoride ions (Zwilling *et al* 1999; Habazaki *et al* 2002; Anitha *et al* 2010). The following equations represent the oxide layer formation (1, 2) and dissolution (3, 4) resulting in nanotubes.



With organic electrolytes, donation of oxygen is more difficult in comparison to water and results in a reduced tendency to form oxide. The reduction in water content allows forma-

tion of thinner or lower quality barrier layers through which ionic transport may be enhanced, due to the faster movement of Ti/TiO₂ interface into the titanium substrate giving rise to tubes (Haripriya *et al* 2007; Shankar *et al* 2007).

The J – V curves of the back illuminated DSSC (figure 5) before TiCl₄ treatment presented a short-circuit current density (J_{sc}) of 2.5 mA/cm², an open-circuit voltage (V_{oc}) of 0.66 V, a fill factor (FF) of 42 % and an overall conversion efficiency (η) of 0.26%. After TiCl₄ treatment, the cell attained an η of 3.5 % with a J_{sc} of 5.7 mA/cm², a V_{oc} of 0.70 V, and FF of 52.41 (%). The J_{sc} and η of the cell was significantly increased through TiCl₄ treatment by 9.5 and 13 times, respectively with a significant improvement in the fill factor. The influence of TiCl₄ treatment for high rate of electron transfer through TiO₂ nanotubes in DSSC is quite well known (Sommeling *et al* 2006). Studies (Charoensirithavorn *et al* 2010) using intensity-modulated photocurrent spectroscopy (IMPS) and intensity-modulated photovoltage spectroscopy (IMVS) have shown that the electron transport time in TiO₂ nanotube treated with TiCl₄ was 3 times faster than their untreated counterparts. This was attributed to the decrease in number of deep trap states existing on the surface of the TiCl₄ treated TiO₂ by surface passivation. Another reason for the improved performance could be attributed to the fact that, on treating with TiCl₄, TiO₂ nanoparticles could nucleate on the surface of the nanotubes, thereby further increasing the surface area and resulting in better dye–TiO₂ interaction. For same dye configuration and 14 μm long TiO₂ nanotubes, Wang and Lin (2010) reported $\eta = 4.34$ % for backside illuminated DSSC. Their study reports 1.7 times increase in η (i.e. 6.36%) after TiCl₄ treatment. Comparing with results, the efficiency reported in this work is quite appealing, since the film thickness is only 1.5 μm and 13 times increase in efficiency is attained after TiCl₄ treatment. This can be attributed to the highly suitable geometric configuration (i.e. good lateral spacing and open

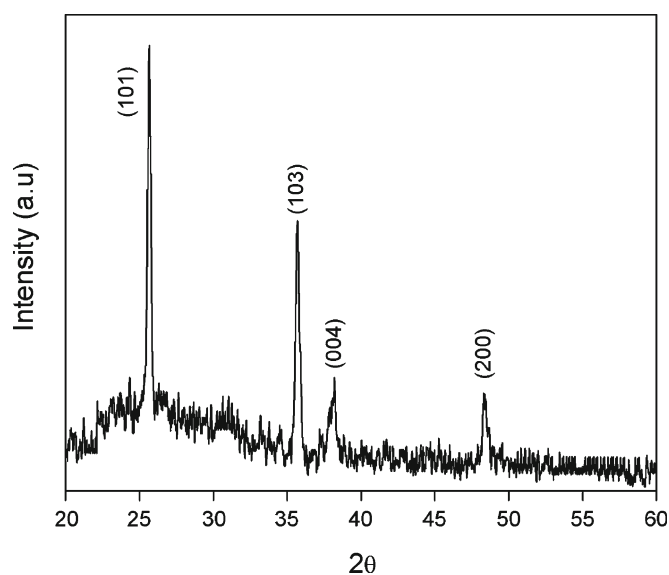


Figure 4. XRD patterns of TiO₂ nanotube layer.

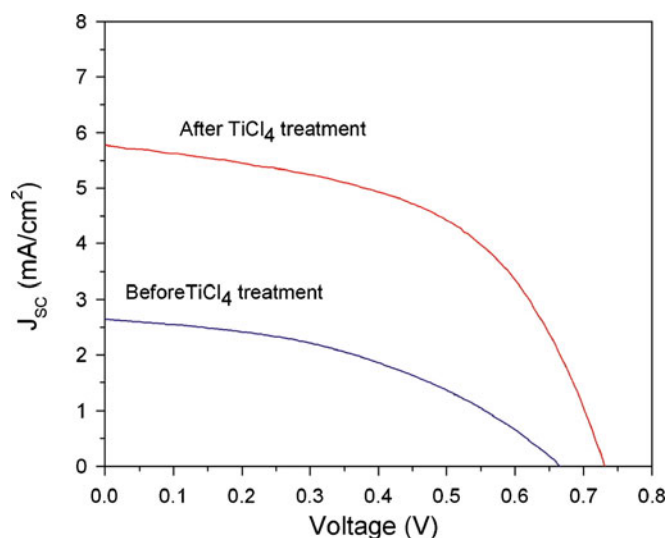


Figure 5. J_{sc} – V characteristics of TiO₂ nanotube based back illuminated DSSC.

Table 1. Comparison of photovoltaic properties of back illuminated DSSC in relation to anodization time and TiO₂ tube morphology.

Sl. No.	Anodization time (h)	Tube length (μm)	Diameter (nm)	Lateral spacing (nm)	J_{sc} (mA/cm ²)	Efficiency (η) %	Fill factor (%)
1	24	1.5 ± 0.3	83 ± 22	65 ± 36	5.3 ± 0.8	3 ± 0.65	51 ± 2
2	36	6.2 ± 1.2	96 ± 35	52 ± 23	4.3 ± 0.6	1.7 ± 0.4	50 ± 3.5
3	48	8.4 ± 1.5	104 ± 41	31 ± 19	3.3 ± 0.5	1.4 ± 0.5	48 ± 1.8
4	72	11.3 ± 2.1	108 ± 54	28 ± 13	1.2 ± 0.3	1.2 ± 0.6	47 ± 2.1

ended tubular structure) of TiO₂ nanotube layer, which after healing of defects by TiCl₄ treatment enhances maximum dye interaction for the shorter nanotubes. Using an extrapolation and based on reported studies (Chen *et al* 2008), we expected that further tuning of the tube geometry, with trend towards slightly longer nanotubes could significantly enhance the cell efficiency. However, this was not the case in the present study. Table 1 shows that with increasing anodization time to different periods of 36, 48 and 72 h there was an average increase in TiO₂ tube length and diameter. It should be noted that all the values reported in Table 1 are for the photo-anodes used after TiCl₄ treatment. It was seen that scattering in the values of tube length and diameter increased with anodization time. This means that new tubes (of lesser diameter and length) were formed in the intertubular lateral spaces resulting in higher scattering of tube length values and reflected as decrease in the lateral spacing values with increasing anodization time. In our case, the short-circuit current density, J_{sc} and efficiency, η values, show a tendency to decrease with increasing tube length. Similar trend was reported recently (Xuan *et al* 2011) where the increment in the short-circuit current density, efficiency and fill factor values decreased with increasing tube length. This decrease was attributed to the decrease in dye-TiO₂ interaction (possibly resulting from reduced lateral spacings between tubes). Besides, longer TiO₂ tubes can present more inherent defects that can enhance electron trapping sites as it attempts to reach the electrode surface (Zhu *et al* 2007; Jennings *et al* 2008).

4. Conclusions

Large-scale, vertically aligned TiO₂ nanotubes were produced on Ti substrate by a controlled anodization technique. The formed TiO₂ nanotubes showed narrowly distributed diameter size (~80 nm) with an average thickness of ~1.5 μm with a broad multi-modal lateral spacing distribution (LSD) between the tubes, indicating that there was good lateral spacing/opening between the nanotubes, which could enhance the dye-TiO₂ interaction. XRD analysis showed the formation of anatase phases. The possibility of employing these TiO₂ nanotubes on Ti substrate as photoanodes in back illuminated dye sensitized solar cells (DSSCs) was demonstrated with an overall efficiency of 0.26%. The efficiency was dramatically improved to 3.5 % by giving simple TiCl₄ treatment to the nanotubes. It was observed that the ave-

rage J_{sc} , η and fill factor values show a tendency to decrease with increasing tube length. This was mainly attributed to the observed decrease in lateral spacings between tubes, which prevented dye percolation within the TiO₂ tubes. Further longer TiO₂ tubes also increases the probability of inherent electron trapping defects thereby decreasing the performance of DSSCs. Thus the present study shows that processing shorter TiO₂ tube lengths with controlled lateral spacings can be promising in further improving the performance of DSSCs.

Acknowledgment

Department of Science and Technology (DST), Government of India, is acknowledged for financial support under the NATAG program monitored by Dr G Sundararajan.

References

- Anitha V C, Menon D, Nair S V and Prasanth R 2010 *Electrochim. Acta* **55** 3703
- Charoensirithavorn P, Ogomi Y, Sagawa T, Hayase S and Yoshikawa S 2010 *J. Electrochem. Soc.* **157** B354
- Chen C -C, Chung H -W, Chen C -H, Lu H -P, Lan C -M, Chen S -F, Luo L, Hung C -S and Diao E W -G 2008 *J. Phys. Chem. C* **112** 19151
- Habazaki H, Uozumi M, Konno H, Shimizu K, Nagata S, Asami K, Skeldon P and Thompson G E 2002 *Electrochim. Acta* **47** 3837
- Haripriya E P, Shankar K, Paulose M, Varghese O K and Grimes C A 2007 *J. Phys. Chem. C* **111** 7235
- Jennings J R, Ghicov A, Peter L M, Schmuki P and Walker A B 2008 *J. Am. Chem. Soc.* **130** 13364
- Liu B, Boercker J E and Aydil E S 2008 *Nanotechnology* **19** 505604
- Park N G, van de Lagemaat J and Frank A J 2000 *J. Phys. Chem.* **B104** 8989
- Paulose M, Shankar K, Varghese O K, Mor G K, Hardin B and Grimes C A 2006 *Nanotechnology* **17** 1446
- Paulose M, Haripriya E P, Varghese O K, Peng L, Popat K C, Desai T A and Grimes C A 2007 *J. Phys. Chem.* **C111** 14992
- Roy P, Kim D, Lee K, Spiecker E and Schmuki P 2010 *Nanoscale* **2** 45
- Shankar K, Gopal K M, Fitzgerald A and Grimes C A 2007 *J. Phys. Chem. C* **111** 21
- Sommeling P M, O'Regan B C, Haswell R R, Smit H J P, Bakker N J, Smits J J T, Kroon J M and Van Roosmalen J A M 2006 *J. Phys. Chem.* **B110** 19191
- Tang Y, Tao J, Zhang Y, Wu T, Tao H and Bao Z 2008 *Acta. Phys.-Chim. Sin.* **24** 2191

- Tao R H, Wu J M, Xue H X, Song X M, Pan X, Fang X Q, Fang X D and Dai S Y 2010 *J. Power Sources* **195** 2989
- Varghese O K, Paulose M and Grimes C A 2009 *Nature Nanotech.* **4** 592
- Wang J and Lin Z 2010 *Chem. Mater.* **22** 579
- Xuan P, Changhong C, Kai Z and Zhaoyang F 2011 *Nanotechnology* **22** 235402
- Zhu K, Neale, N R, Miedaner A and Frank A J 2007 *Nano. Lett.* **7** 69
- Zwilling V, Darque-Ceretti E, Boutry-Forveille A, David D, Perrin M Y and Aucouturier M 1999 *Surf. Interf. Anal.* **27** 629